Modeling of polycrystalline ZnO thin-film transistors with a consideration of the deep and tail states*

Gao Hai-Xia(高海霞)†, Hu Rong(胡 榕), and Yang Yin-Tang(杨银堂)

School of Microelectronics, Xidian University, Xi'an 710071 *China*

(Received 13 April 2011; revised manuscript received 30 June 2011)

We report a model of the carrier transport and the subgap density of states in a polycrystalline ZnO film for simulating a polycrystalline ZnO thin film transistor. This simple model considering the deep and the band tail states reproduces well the characteristics of polycrystalline ZnO thin film transistors. Furthermore, using the developed model, we study the effects of defect parameters on the electrical performances of the polycrystalline ZnO thin film transistors.

Keywords: modeling, ZnO thin film transistor, deep state, band tail

PACS: 68.60.–p, 73.50.–h, 73.61.–r **DOI:** 10.1088/1674-1056/20/11/116803

1. Introduction

Oxide semiconductors, such as zinc oxide (ZnO), indium gallium zinc oxide (IGZO) and indium tin oxide (ITO), have received considerable attention due to their potential applications and interesting properties, which include its low-temperature process, transparency, good stability and large-area uniformity.[1−3] Among those materials, ZnO has the simplest composition and a relatively low cost. The polycrystalline ZnO (poly-ZnO) thin film is composed of nano grains with grain sizes ranging from 10 nm to 100 nm. The grain boundaries (GBs) can be deposited using many growth techniques including sputtering,[4] molecular beam epitaxy (MBE),[5] pulse laser deposition[6] and metal-organic chemical vapour deposition (MOCVD).[7] Those small grains and dense GBs result in a semi-insulating film, which is necessary for the enhancement-mode thin film transistor (TFT) fabrication.

Despite the rapid improvement of the ZnO TFT performance, many physical properties of the ZnO TFT are still not well understood. There are only a limited number of publications related to the modeling and simulation of ZnO TFTs.[8−10] Although a model to explain the fundamental transport properties of poly-ZnO TFTs based on the mid-gap deep states has been investigated,[9] the model cannot reproduce well the characteristics of poly-ZnO TFTs in the above-threshold region. The above-threshold characteristics of the silicon-based TFTs have been found to strongly depend on the band tail states.[11] Amorphous IGZO TFT models using the density of states containing both the tail and the deep gap states have been developed, and they reproduce well the characteristics of the amorphous IGZO TFTs.[12] In this paper, we report a model of the poly-ZnO TFTs based on the tail and the deep states, which can reproduce well the characteristics of the poly-ZnO TFTs in both the sub-threshold and the above-threshold regions.

2. Modeling

Figure 1 shows the device structure used in the modeling. The transistors to be modeled were fabricated on heavily doped silicon substrates, which were used as the gate electrodes as well. The gate dielectric was a thermally grown SiO_2 layer. The thickness of the channel layer processed using radio frequency (RF) sputtering at room temperature was controlled by an alpha step. After the channel layer, the source and the drain Al electrodes were deposited by vacuum evaporation and then appropriately etched. The detailed fabrication information about the ZnO TFT can be found in the literature.[13] The experimentally optimized dimensions (channel length $L = 35$ μm, channel width $W = 2$ mm and gate oxide thickness $t_{SiO2} = 280$ nm) were used to achieve the best TFT performance. In this paper, we study the transistors with channel layer thicknesses t_{ZnO} of 15 nm, 25 nm, 50 nm and 70 nm, which are labeled as TFT A, TFT

*Project supported by the Fundamental Research Funds for the Central Universities, China (Grant No. K50510250001).
†Corresponding author. E-mail: hxgao@mail.xidian.edu.cn
© 2011 Chinese Physical Society and IOP Publishing Ltd

B, TFT C and TFT D, respectively, for convenience in the following.

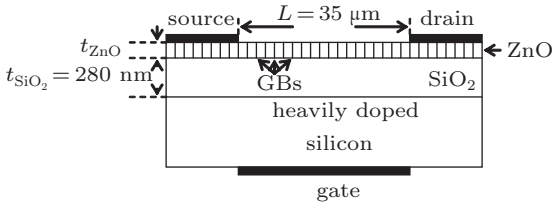


Fig. 1. Device structure used in modeling ZnO TFT.

For our modeling and simulation study, a commercially available device simulator ATLAS[14] was used. In the device simulator, we specified ZnO as the active channel layer material. The ZnO thin film was defined by many 15/25/50/70 nm thick nano grains and the GBs between them. The GB was modeled as a thin semiconductor layer having defect states parallel to the ZnO film thickness, and the regions on both sides of the GBs were assumed to be completely defect-free. All necessary material constants of ZnO are listed in Table 1.

Table 1. Material constants of ZnO for device simulation.

Parameter	Value
Energy gap at 300 K	3.4 eV
Beta coefficient for temperature dependence of bandgap	920 K
Alpha coefficient for temperature dependence of bandgap	8×10^{-4} eV/K
Dielectric constant	8.12
Saturation velocity for the electric field dependent mobility	3.2×10^{-7} cm/s
Low-field electron mobility	150 $cm^2/V{\cdot}s$
Electron affinity	4.29 eV
Donor level	0.03 eV
Donor concentration	5×10^{16} cm^{-3}

The density of the defect states (DOS) $g(E)$, which dominates the properties of amorphous or polycrystalline TFTs, was specified as a combination of four parameterized components:[15] an acceptor-like exponential band tail function $g_{\rm TA}(E)$, a donor-like exponential band tail function $g_{\rm TD}(E)$, an acceptor-like Gaussian deep state function $g_{\rm GA}(E)$ and a donor-like Gaussian deep state function $g_{\rm GD}(E)$, where E denotes the state energy. As ZnO in this work was an n-type semiconductor and the ZnO TFTs operated in the n-channel mode, we considered only the acceptor-like states. Finally, $g(E)$ is given as

$$g(E) = g_{\rm GA}(E) + g_{\rm TA}(E), \tag{1}$$

$$g_{\rm GA}(E) = N_{\rm GA} \cdot \exp\left[-\left(\frac{E_{\rm GA} - E}{W_{\rm GA}}\right)^2\right], \tag{2}$$

$$g_{\rm TA}(E) = N_{\rm TA} \cdot \exp\left(\frac{E - E_{\rm c}}{W_{\rm TA}}\right), \tag{3}$$

where $E_{\rm GA}$ denotes the peak energy, $N_{\rm GA}$ is the density at the peak energy and $W_{\rm GA}$ is the characteristic decay energy for the Gaussian distribution of $g_{\rm GA}(E)$. For the exponential distribution of $g_{\rm TA}(E)$, $E_{\rm c}$ is the conduction band edge, $N_{\rm TA}$ is the conduction band edge intercept density, and $W_{\rm TA}$ is the characteristic decay energy.

We used the drift-diffusion (DD) simulation model, in which the basic equations used are similar to those used for a single-crystal device except that the trapped charge is included in the Poisson's equation and a modified Shockley–Read–Hall (SRH) recombination term is used in the carrier continuity equations. Also, we employed the band-to-band tunneling model to deal with the off-state carrier transport.

3. Results and discussion

Figures 2(a)–2(d) respectively show the fitting results to the experimental data[13]under a drain–source voltage ($V_{\rm DS}$) of 30 V. In the figures, $I_{\rm DS}$ is the drain current and $V_{\rm GS}$ is the gate voltage. According to Fig. 2, TFT B and TFT C each have a better surface morphology and a large saturation current, although their grain sizes are smaller. The saturation current of the device is mainly determined by the surface property of the ZnO film rather than its grain size.[13] From the fittings, we can see that the model reproduces the experimental data well. The optimized fitting defect parameters are listed in Table 2.

The $N_{\rm TA}$ parameters shown in Table 2 are at 10^{21} order of magnitude, which are similar to that in a-Si:H.[16] It is necessary to discuss the influence of the tail states on the performance of the poly-ZnO TFT. The tail states near the conduction band edge are due to the microscopic disorders in the material network.[17] In the poly-ZnO film, due to the insufficient crystallization during the low-temperature process, the actual grain size is generally below 100 nm, which is much smaller than the general grain size in the poly-silicon material[18] and will strengthen the disorders in the ZnO network greatly. As the degree of the microscopic disorder increases, the density of the tail states is increased, and the effect of the tail states on the transistor characteristics becomes stronger.

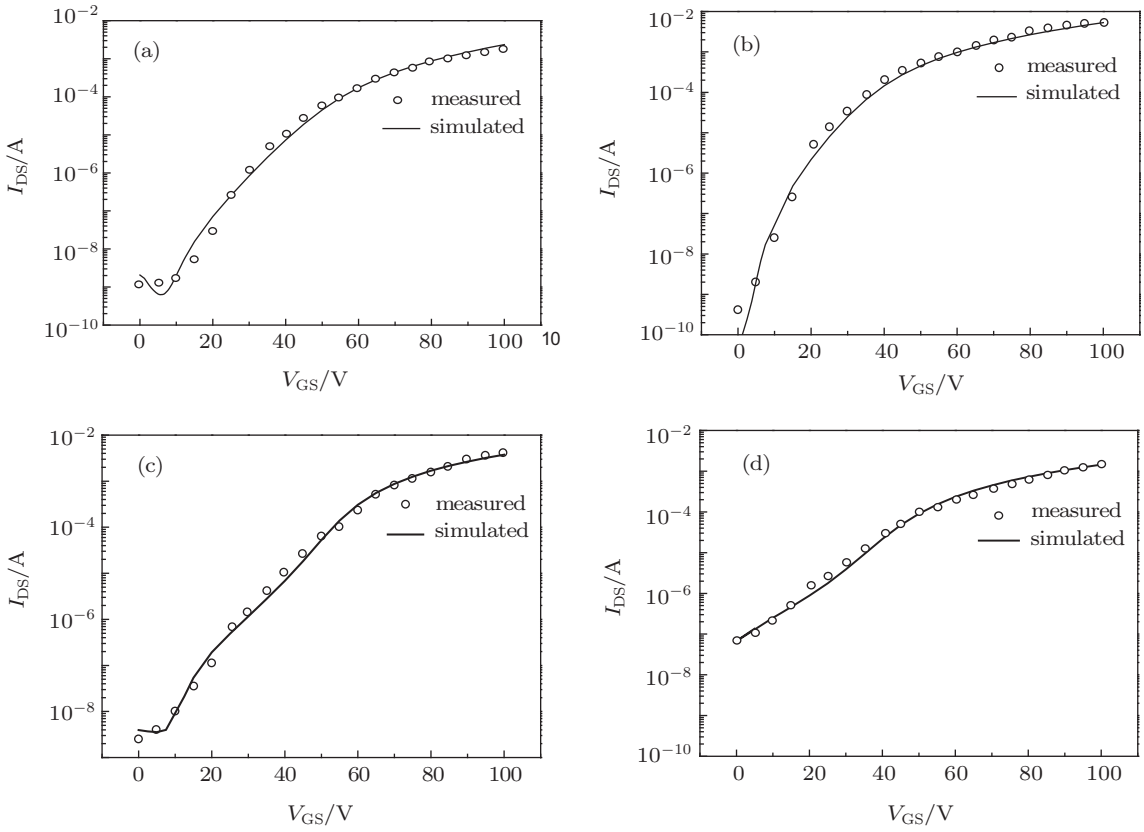


Fig. 2. Simulation and measurement results of (a) TFT A with a thickness of 15 nm, (b) TFT B with a thickness of 25 nm, (c) TFT C with a thickness of 50 nm, and (d) TFT D with a thickness of 70 nm.

Table 2. Defect parameters.

Device	TFT A	TFT B	TFT C	TFT D
Film thickness/nm	15	25	50	70
RMS/nm	5.43	1.89	2.82	6.5
Grain size/nm	60	30	35	55
GB width/nm	2	1	1	2
E_{GA}/eV	1.7	1.7	1.7	1.7
W_{GA}/eV	0.33	0.28	0.3	0.3
$N_{GA}/10^{19}$ cm$^{-3}\cdot$eV^{-1}	5.8	4	7.3	2
W_{TA}/eV	0.117	0.12	0.145	0.145
$N_{TA}/10^{21}$ cm$^{-3}\cdot$eV^{-1}	2.7	3.6	3	3
a_{bb} /cm$^{-1}\cdot$V$^{-2}\cdot$s^{-1}	2×10^{16}	1×10^{12}	7×10^{14}	–
$b_{bb}/10^7$ V$\cdot$cm^{-1}	5.5	6.5	6.5	–
QF/10^{12} cm^{-2}	1.4	1.3	2	2.8

It was mentioned in Ref. [13] that the root mean square (RMS) values of the ZnO film surfaces of TFT A, TFT B, TFT C and TFT D were 5.43 nm, 1.89 nm, 2.82 nm and 6.5 nm, respectively. In our paper, we characterize the RMS difference by the fixed oxide charge density (QF), which is the interface charge at the ZnO/SiO_2 boundary. According to Table 2, with the active layer thickness increasing from 25 nm to 70 nm, the interface charge increases from 1.3×10^{12} cm^{-2} to 2.8×10^{12} cm^{-2}. Parameters a_{bb} and b_{bb} in Table 2 are the user-definable parameters in the band-to-band tunneling model, which are adjusted during our simulation to reproduce well the off-state current. The difference between the parameters of tunnel is reasoned by the differences in the surface morphology and the thickness of the channel.

To probe the reliability of the modeling and the influence of each DOS parameter (N_{TA}, W_{TA}, N_{GA}, and W_{GA}) on the device characteristics, the transfer characteristics of the poly-ZnO TFT were simulated. In each panel of Fig. 3, only one DOS parameter is varied, while the other parameters are kept the same as those listed in Table 2.

Figures 3(a) and 3(b) show the simulated transfer characteristics of the ZnO TFT when parameters N_{TA} and W_{TA} are changed, respectively. The dependence of parameter N_{TA}/W_{TA} on the on-current and the subthreshold swing is strong. With the increase of parameterN_{TA}/W_{TA}, the on-current decreases, and the subthreshold swing rises greatly, which prove that it is necessary to consider the effect of the band tail on the GB model of the ZnO TFT for an improvement of accuracy. In n-channel TFTs, when the applied gate voltage is less than the threshold voltage, the quasi-

electron Fermi level lies within the acceptor-like deep states, which results in the strong dependence of the threshold voltage on the parameter of the deep state, such as $N_{\rm GA}$ and $W_{\rm GA}$. As the applied gate voltage increases, the transistor enters into the above threshold voltage operating conditions and the Fermi level moves towards the conduction band lying within the acceptor-like tail states. Due to their higher concentration, the influence of the tail states becomes dominant compared with that of the deep states.

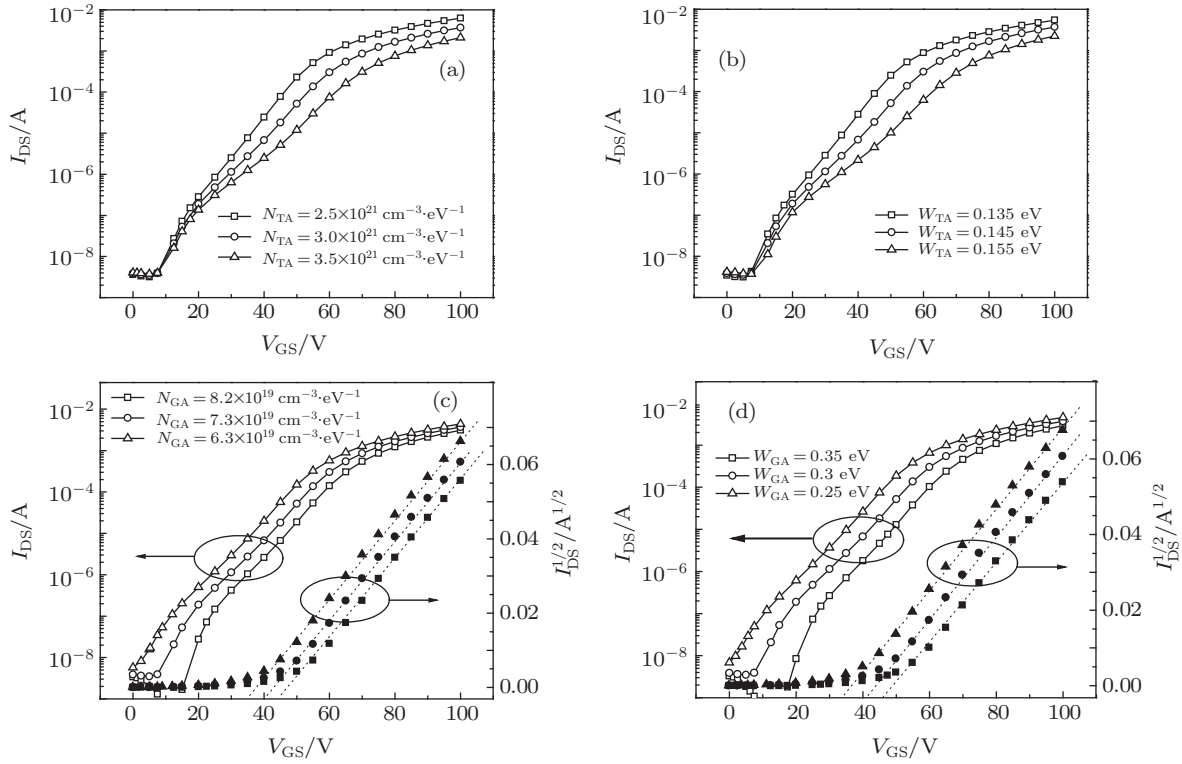


Fig. 3. Influence of DOS parameters (a)$N_{\rm TA}$, (b)$W_{\rm TA}$, (c)$N_{\rm GA}$, and (d)$W_{\rm GA}$ on transfer characteristics of TFT C ($V_{\rm DS}=30$ V).

Figures 3(c) and 3(d) show the results of the simulation for different values of deep state parameters $N_{\rm GA}$ and $W_{\rm GA}$. To study the dependence of the deep state on the threshold voltage and the mobility explicitly, the $I_{\rm DS}^{1/2}$–$V_{\rm DS}$ curves are also shown in the figures. It is well known that the threshold voltage and the subthreshold performance of TFTs are related to the number of the deep state. It is indicated that the deep states are influenced by the subthreshold and the turn-on voltages, the latter is defined as the voltage at which the drain current increases sharply. It is interesting that the mobility is independent of the deep state parameter. The deep state parameters $N_{\rm GA}$ and $W_{\rm GA}$ mainly influence the subthreshold part performance, and the tail state parameters $N_{\rm TA}$ and $W_{\rm TA}$ mainly affect the above-threshold part performance.

4. Conclusion

In this paper, a model of poly-ZnO TFT considering the deep and the tail states in the grain boundary regions is proposed, which can reproduce the ZnO TFT transfer characteristic well, including the subthreshold and the above-threshold performances. In order to verify our conclusion, we simulate four samples with channel layer thicknesses of 15 nm, 25 nm, 50 nm and 70 nm with the proposed model and compare their differences. The dependence of the TFT performance on the parameters of the deep and the tail states is analysed. We find that the deep state mainly affects the subthreshold characteristic, while the tail state influences the above-threshold characteristic, which is due to the position of the Fermi level in the energy band. The model we proposed in this paper shall be generally useful for designing poly-ZnO TFT devices and circuits.

References

[1] Jeon S J, Chang J W, Choi K S, Kar J P, Lee T I and Myoung J M 2011 *Materials Science in Semiconductor Processing* In Press

[2] Lu A, Sun J, Jiang J and Wan Q 2009 *Appl. Phys. Lett.* **95** 222905

[3] Jeong J K 2011 *Semicond. Sci. Tech.* **26** 034008

[4] Furuta M, Kamada Y, Kimura M, Hiramatsu T, Matsuda T, Li C, Furuta H, Fujita S and Hirao T 2010 *IEEE Electron Device Lett.* **31** 1257

[5] Xiu F X, Yang Z, Mandalapu L J, Zhao D T, Liu J L and Beyermann W P 2005 *Appl. Phys. Lett.* **87** 152101

[6] Shin P, Aya Y, Ikegami T and Ebihara K 2008 *Thin Solid Films* **516** 3767

[7] Jia C, Chen Y, Liu G, Liu X, Yang S and Wang Z 2008 *J. Crystal Growth* **311** 200

[8] Zhou Y M, He Y G, Lu A X and Wan Q 2009 *Chin. Phys.* B 18 3966

[9] Hossain F M, Nishii J, Takagi S, Ohtomo A, Fukumura T, Fujioka H, Ohno H, Koinuma H and Kawasaki M 2003 *J. Appl. Phys.* **94** 7768

[10] Zhang A, Zhao X R, Duan L B, Liu J M and Zhao J L 2011 *Chin. Phys.* B 20 057201

[11] Dosev D 2003 *Solid-State Electronics* **47** 1917

[12] Hsieh H H, Kamiya T, Nomura K, Hosono H and Wu C C 2008 *Appl. Phys. Lett.* **92** 133503

[13] Zhang L, Zhang H, Bai Y, Ma J W, Cao J, Jiang X Y and Zhang Z L 2008 *Solid State Commun.* **146** 387

[14] 2007 *ATLAS User's Manual*

[15] Fung T C, Chuang C S, Chen C, Abe K, Cottle R, Townsend M, Kumomi H and Kanicki J 2009 *J. Appl. Phys.* **96** 10

[16] O'Leary S K 2004 *J. Mater. Sci-Mater El.* **15** 401

[17] Takechi K, Nakata M, Eguchi T, Yamaguchi H and Kaneko S 2009 *IEEE Tran. Electron Devices* **56** 2165

[18] Hara A and Sato T 2010 *Jpn. J. Appl. Phys.* **49** 010203